JOURNAL OF GEOPHYSICAL RESEARCH, VOL. 115, A07103, doi:10.1029/2009JA015039, 2010

Click Here for Full Article

Interplanetary circumstances of quasi-perpendicular interplanetary shocks in 1996–2005

I. G. Richardson[1,2] and H. V. Cane[1,3]

Received 29 October 2009; revised 18 February 2010; accepted 9 March 2010; published 10 July 2010.

[1] The angle (θ_{Bn}) between the normal to an interplanetary shock front and the upstream magnetic field direction, though often thought of as a property "of the shock," is also determined by the configuration of the magnetic field immediately upstream of the shock. We investigate the interplanetary circumstances of 105 near-Earth quasi-perpendicular shocks during 1996–2005 identified by $\theta_{Bn} \geq 80°$ and/or by evidence of shock drift particle acceleration. Around 87% of these shocks were driven by interplanetary coronal mass ejections (ICMEs); the remainder were probably the forward shocks of corotating interaction regions. For around half of the shocks, the upstream field was approximately perpendicular to the radial direction, either east-west or west-east or highly inclined to the ecliptic. Such field directions will give quasi-perpendicular configurations for radially propagating shocks. Around 30% of the shocks were propagating through, or closely followed, ICMEs at the time of observation. Another quarter were propagating through the heliospheric plasma sheet (HPS), and a further quarter occurred in slow solar wind that did not have characteristics of the HPS. Around 11% were observed in high-speed streams, and 7% in the sheaths following other shocks. The fraction of shocks found in high-speed streams is around a third of that expected based on the fraction of the time when such streams were observed at Earth. Quasi-perpendicular shocks are found traveling through ICMEs around 2–3 times more frequently than expected. In addition, shocks propagating through ICMEs are more likely to have larger values of θ_{Bn} than shocks outside ICMEs.

Citation: Richardson, I. G., and H. V. Cane (2010), Interplanetary circumstances of quasi-perpendicular interplanetary shocks in 1996–2005, *J. Geophys. Res.*, *115*, A07103, doi:10.1029/2009JA015039.

1. Introduction

[2] In particular in discussions of energetic particle acceleration, interplanetary shocks are often classified in terms of θ_{Bn}, the angle between the shock normal and upstream magnetic field since this parameter is expected to influence the mechanism of particle acceleration at the shock. At quasi-parallel ($\theta_{Bn} \sim 0°$) and intermediate shocks, particles are accelerated by diffusive shock acceleration, a first-order Fermi process in which particles are accelerated by scattering between converging scattering centers upstream and downstream of the shock [e.g., *Toptyghin*, 1980; *Lee*, 1983]. At a quasi-perpendicular shock ($\theta_{Bn} \sim 90°$), "shock drift" acceleration takes place [e.g., *Sarris and Van Allen*, 1974; *Decker*, 1983; *Erdös and Balogh*, 1994]. In this process (see reviews by *Toptyghin* [1980], *Armstrong et al.* [1985], and *Forman and Webb* [1985]), particles drift along the shock front, due to the magnetic field gradient across the shock, in the direction of the $-v \times B$ electric field at the shock front. The distinction between these two acceleration mechanisms may be blurred however. For example, particles can be returned to a quasi-perpendicular shock by magnetic field irregularities, ripples in the shock front or looped magnetic field lines such that the process also has characteristics of diffusive shock acceleration [e.g., *Decker*, 1983, 1990, 1993; *Erdös and Balogh*, 1993, 1994; *Neugebauer and Giacalone*, 2005]. The role of θ_{Bn} in shock acceleration has gained renewed interest with the recent suggestion that compositional variations in solar energetic particle events may be related to differences in θ_{Bn} of the accelerating shocks [*Tylka and Lee*, 2006].

[3] Although θ_{Bn} is often considered to be a property "of the shock," this angle is also determined by the changing direction of the upstream interplanetary magnetic field (IMF) which may be influenced by features ranging in size from waves and turbulence to the large-scale Archimedian spiral structure of the IMF [*Parker*, 1958]. For example, θ_{Bn} would be expected to increase with increasing heliocentric distance for a ~spherical shock driven by a fast interplanetary coronal mass ejection (ICME, the interplanetary manifestation of a coronal mass ejection at the Sun) moving out radially through a Parker spiral field, reaching ~45° at 1 AU (cf. the Helios spacecraft observations of interplanetary

[1]Astroparticle Physics Laboratory, NASA Goddard Space Flight Center, Greenbelt, Maryland, USA.
[2]CRESST and Department of Astronomy, University of Maryland, College Park, Maryland, USA.
[3]Physics Department, University of Tasmania, Hobart, Tasmania, Australia.

Copyright 2010 by the American Geophysical Union.
0148-0227/10/2009JA015039

shocks at 0.3–1 AU reported by *Volkmer and Neubauer* [1985]). Evidently, to produce a quasi-perpendicular configuration at 1 AU, the magnetic field direction upstream of such a shock must deviate considerably from the Parker spiral field. Another possibility is that the ICME-driven shock is strongly "draped" around the ICME, resulting in a quasi-perpendicular configuration on the western flank of the shock, where the shock front is approximately aligned with the spiral IMF. Although cartoons of interplanetary shocks often show this strong draping [e.g., *Hundhausen*, 1972, Figure 2], observations [e.g., *Cane*, 1988] suggest that these shocks are typically near-spherical with only modest draping at the flanks. In this case, θ_{Bn} would not be expected to vary strongly with location along a shock moving through a spiral magnetic field.

[4] In this study, we focus on the interplanetary circumstances of a sample of 105 quasi-perpendicular shocks observed in the near-Earth solar wind in 1996–2005, a period extending from the preceding minimum through to the late decay phase of solar cycle 23. A novel feature of this study is that we have identified these shocks using estimates of θ_{Bn} inferred from in-situ plasma and magnetic field data and by examining energetic (~1 MeV/n) ion observations for evidence of shock drift acceleration. We examine the types of solar wind structures through which these shocks were propagating at the time of observation and consider whether certain types of structures may favor the formation of such shocks.

2. Identification of Quasi-perpendicular Shocks

2.1. Using Plasma/Field Data

[5] We have used shock identifications and values of θ_{Bn} from several sources. One source is the shock database compiled by Justin Kasper (Harvard-Smithsonian Center for Astrophysics; http://www.cfa.harvard.edu/shocks/). This combines the results of several independent shock analysis methods to arrive at a consensus of the shock parameters. The data used are principally from the WIND spacecraft with additional data from the Advanced Composition Explorer (ACE) spacecraft. The Kasper database provides parameters for shocks during 1995 to 2004 but is not complete. In particular, only shocks in 2003 and 2004 associated with intense geomagnetic storms [*Zhang et al.*, 2007] are included. To complement this database, we used the ACE shock list (http://www.ssg.sr.unh.edu/mag/ace/ACElists/obslist.html) compiled by C. W. Smith (University of New Hampshire). Parameters obtained from interactive and automated fits are provided for shocks up to October 2005 at the time of writing. In general we use here the interactive fits, unless the automated fit has a substantially smaller error in θ_{Bn}. We have also referred to the WIND shock list of *Berdichevsky et al.* [2000].

[6] We have chosen to define "quasi-perpendicular" shocks as fast forward shocks (i.e., we do not consider slow forward shocks or reverse shocks) with $\theta_{Bn} \geq 80°$. Tables 1 and 2 include the shocks in 1996–2005 that meet this criterion in any of the shock lists discussed above (additional shocks in Tables 1 and 2 will be discussed below). The time of shock passage is listed in the first column of Tables 1 and 2. If the shock is accompanied by a geomagnetic storm sudden commencement (SSC; provided by the National Geophysical Data Center), we give the SSC time, indicated by "S". Otherwise, the time given is at WIND, ACE or IMP 8 as indicated by 'W', 'A', or 'I', respectively. Typically a shock is identified at multiple spacecraft but only one time is listed due to space limitations. The value of θ_{Bn} from the Kasper database is given in column two. In the third column, values of θ_{Bn} from the ACE shock list are enclosed in parentheses while those in square brackets are from *Berdichevsky et al.* [2000] using WIND data.

[7] For each shock in Tables 1 and 2, we give our assessment of the shock type, i.e., whether the shock was generated by a CIR or an ICME (not to be confused with the structure upstream of the shock to be discussed in following sections). CIRs are formed by the interaction of high speed solar wind streams from coronal holes with the preceding slower solar wind and are identified from the characteristic variations in their plasma parameters [e.g., *Belcher and Davis*, 1971; *Richardson*, 2004, and references therein]. Expansion of the CIR may lead to the formation of a forward shock at the CIR leading edge. Though CIR shocks typically form beyond 2 AU [e.g., *Smith and Wolfe*, 1976, 1977], they may develop at or within 1 AU [e.g., *Schwenn*, 1990; *Berdichevsky et al.*, 2000].

[8] To identify shocks driven by ICMEs, we have referred to our "comprehensive" list of ICMEs since 1996 (http://www.ssg.sr.unh.edu/mag/ace/ACElists/ICMEtable.html) that is updated from the list from *Cane and Richardson* [2003] and includes shock associations. Since the flanks of ICME-driven shocks typically extend beyond the related ICME [e.g., *Borrini et al.*, 1982; *Cane*, 1988; *Richardson and Cane*, 1993] some ICME-driven shocks will not be followed by an ICME observed in situ. In general, if a shock is not followed by an ICME and does not appear to be associated with a CIR, we assume it is the flank of an ICME-associated shock. In a few cases, the assignment is uncertain.

2.2. Using Energetic Particle Data

[9] To provide an independent method of identifying a sample of quasi-perpendicular shocks, we have examined energetic particle data from various spacecraft instruments in the vicinity of all ~350 forward shocks during our study period for evidence of shock drift acceleration. This process increases the component of the particle velocity perpendicular to the magnetic field direction, resulting in a "pancake" angular distribution in the particles transmitted downstream in which the particle intensity at a given energy is greatest for pitch angles ~perpendicular to the field [e.g., *Sarris and Van Allen*, 1974; *Marhavilas et al.*, 2003]. The accelerated particles also tend to be localized at the shock front, forming short duration "spike-like" intensity increases close to shock passage that typically extend to energies of ~5 MeV and have softer spectra than the ambient ions [e.g., *Sarris and Van Allen*, 1974; *Sarris et al.*, 1976; *Decker*, 1983; *Sarris and Krimigis*, 1985].

[10] To search for pancake ion distributions, we used data from the Goddard Medium Energy instrument (GME) on IMP 8 [*McGuire et al.*, 1986] which provided observations of protons and heavy ions at energies of ~0.5 to 400 MeV/n from October 1973 until October 2006. In particular, we examined observations of 0.5–4 MeV/n proton and He ion anisotropies made by accumulating particle counts in 8 azi-

Table 1. Solar Wind Structures Associated With "Quasi-perpendicular" Shocks in 1996–2000

Shock[a]					~1 MeV[c]		
Date(UT)	θ_{B_n}(°) Kasper	θ_{B_n}(°) [WIND](ACE)	Type	Structure[b]	Spike?	Pancake?	Upstream Field Direction
1996 Apr 08 1334S	84 ± 5	[67 ± 2]	C	HPS	n	…	Spiral
1996 Jun 18 2235W	…	[87 ± 3]	C	SSW	n	…	E–W
1997 Mar 20 1942W	81 ± 8	[84 ± 13]	C?	HPS	n	…	W–E
1997 Apr 10 1258W	65 ± 20	[85 ± 5]	I	HPS	Y	…	Spiral, N
1997 May 15 0159S	85 ± 4	[86 ± 2]	I	HPS	Y	0145 – >0215	Spiral
1997 May 25 1434S	84 ± 5	[80 ± 10]	I	SSW	n	…	W–E, N
1997 Oct 10 1612S	86 ± 4	…	I	ICME	Y	…	W–E
1997 Oct 24 1050S	61 ± 12	…	C?	HPS	Y	…	E–W
1997 Nov 06 2248S	…	…	I	HPS	Y	n	W–E
1997 Nov 22 0949S	83 ± 3	…	I	HPS	Y	…	W–E
1997 Dec 30 0209S	71 ± 9	…	I	HPS	Y	…	E–W
1998 Jan 06 1416S	74 ± 14	…	I	HPS	Y	1400–1430	E–W
1998 Jan 24 0529S	51 ± 19	…	C?	HPS	Y	…	Spiral
1998 Mar 04 1156S	45 ± 14	(88 ± 3)	I	SSW	n	…	S
1998 Apr 07 1749S	40 ± 12	…	I?	HPS	n	1715–1800	Radial
1998 May 04 0230A	…	(79 ± 5)	I	ICME	Y		⊥ Spiral
1998 Aug 06 0736S	81 ± 1	(82 ± 3)	I	ICME?	Y	0730–1000	W–E, S
1998 Aug 26 0655I	68 ± 20	(88 ± 2)	I	SSW	Y	…	N
1998 Oct 23 1302I	37 ± 15	(56 ± 12)	I	hss	Y	1200–1345	N
1998 Nov 08 0451S	52 ± 11	(76 ± 2)	I	ICME	Y	…	W–E
1998 Dec 11 1930A	…	(83 ± 4)	?	HPS	Y	…	E–W
1998 Dec 26 0956W	78 ± 8	(82 ± 6)	I	hss	Y	…	N
1999 Jan 13 1054S	61 ± 9	(59 ± 7)	C	HPS	Y	…	S
1999 Feb 17 0709S	85 ± 4	(80 ± 6)	I	ICME	Y	…	W–E, S
1999 Mar 10 0130S	82 ± 5	(78 ± 4)	I	HPS	n	…	E–W, S
1999 Jun 26 0325S	86 ± 3	…	I?	HPS	n	n	Spiral
1999 Aug 04 0219S	52 ± 7	(44 ± 23)	I	ICME TE?	n	0115–0230	Spiral
1999 Aug 23 1541W	85 ± 4	(58 ± 4)	C	ICME TE	n	…	W–E
1999 Sep 22 1222S	77 ± 10	(64 ± 7)	I	HPS	Y	1230–1330	⊥ Spiral, N
1999 Oct 21 0225S	69 ± 5	(77 ± 3)	I	HPS	Y	n	W–E
1999 Oct 28 1216S	62 ± 14	(83 ± 4)	I?	SSW	n	…	⊥ Spiral, N
1999 Nov 13 1246I	67 ± 6	(88 ± 2)	I	ICME	n	…	W–E, S
2000 Feb 05 1544S	70 ± 7	(90 ± 8)	C	SSW	n	…	Spiral
2000 Feb 11 2352S	84 ± 5	(88 ± 3)	I	ICME TE?	Y	2345–0000	Spiral
2000 Feb 20 2139S	86 ± 2	(85 ± 3)	I	SSW	Y	…	W–E
2000 Apr 06 1632W	66 ± 4	(71 ± 2)	I	HPS?	Y	…	Spiral
2000 May 23 2342W	63 ± 18	…	I	ICME	Y	2330–0000	N
2000 Jul 10 0638S	67 ± 7	(67 ± 6)	I	SSW	Y	…	W–E, S
2000 Jul 11 1206I	69 ± 5	(84 ± 3)	I	ICME	n	1200–1245	W–E
2000 Jul 19 1527S	58 ± 9	(81 ± 7)	I	hss	Y	…	Spiral
2000 Jul 26 1857S	85 ± 3	(84 ± 4)	I	Sheath?	n	1900–1915	Spiral, S
2000 Jul 28 0634S	53 ± 6	(51 ± 8)	I	ICME TE	Y	0700–0815	W–E
2000 Jul 28 0909A	47 ± 8	(60 ± 4)	I	Sheath	Y	n	⊥ Spiral
2000 Aug 10 0501S	81 ± 8	(18 ± 9)	I	SSW	n	…	Spiral
2000 Aug 11 1846S	79 ± 7	(61 ± 5)	I	ICME/MC	Y	Y[d]	Spiral
2000 Sep 06 1701S	67 ± 6	(85 ± 3)	I?	SSW	Y	…	W–E, N
2000 Sep 17 1657A	54 ± 22	(73 ± 19)	I	hss	Y	…	N
2000 Sep 30 1116W	60 ± 11	(86 ± 10)	?	HPS	n	…	W–E
2000 Oct 05 0322I	74 ± 5	(66 ± 8)	I	ICME/MC	Y	0330–0445	S
2000 Oct 12 2228S	73 ± 5	(83 ± 6)	I	SSW	Y	…	Spiral
2000 Nov 04 0221S	73 ± 16	(84 ± 3)	C	HPS	Y	0230–0315	Spiral
2000 Nov 26 1158S	52 ± 21	(83 ± 7)	I	Sheath	Y	n	W–E, N

[a]Shock time: S, storm sudden commencement time; W, time of passage at WIND; A, time at ACE, and I, time at IMP 8. θ_{Bn} in column 2 is from the Kasper database, generally at WIND. Values of θ_{Bn} in column 3 in square brackets are WIND values from *Berdichevsky et al.* [2000], while those in parentheses are from the ACE shock list. Shock type C (I) denotes a CIR (ICME-driven) shock.

[b]Structure through which the shock is propagating at the time of observation: "HPS," heliospheric plasma sheet; "ICME," interplanetary coronal mass ejection ("/MC" indicates a magnetic cloud); "hss," high-speed stream from a coronal hole; "Sheath," sheath between an ICME and the related upstream shock; "ICME TE," at or closely following the trailing edge of an ICME.

[c]Evidence of shock-drift acceleration in ~1 MeV ions: "…," low intensity or data gap; "Y," evidence of ion intensity spike in the vicinity of shock passage. "n," observations available but feature is not evident. Times of pancake distributions observed by the IMP 8 GME are given.

[d]SOHO/ERNE observation from *Torsti et al.* [2006].

Table 2. Solar Wind Structures Associated With "Quasi-perpendicular" Shocks in 2001–2005

Shock[a]					~1 MeV[c]		
Date(UT)	θ_{B_n}(°) Kasper	θ_{B_n}(°) [WIND](ACE)	Type	Structure[b]	Spike?	Pancake?	Upstream Field Direction
2001 Jan 23 1048S	39 ± 7	(24 ± 23)	I	SSW	Y	…	Radial
2001 Mar 03 1121S	32 ± 17	(82 ± 4)	I	SSW	n	…	Spiral, S
2001 Mar 27 1747S	59 ± 10	(49 ± 22)	I	Sheath	Y	…	Spiral
2001 Mar 31 0052S	77 ± 14	(75 ± 2)	I	ICME TE	Y	0115–0300	W–E, S
2001 Apr 08 1101S	56 ± 18	(90 ± 3)	I	Sheath	Y	…	W–E
2001 Apr 18 0046S	66 ± 22	(81 ± 5)	I	SSW	n	n	E–W
2001 Apr 28 0500S	54 ± 15	(88 ± 2)	I	hss?	Y	n	W–E
2001 May 12 1003W	62 ± 8	(84 ± 4)	I	SSW	Y	0945–1015	⊥ Spiral, S
2001 Jun 18 0259S	79 ± 12	…	C	HPS	Y	…	Spiral
2001 Aug 17 1103S	85 ± 3	(62 ± 6)	I	SSW	Y	…	N
2001 Aug 27 1952S	45 ± 11	(89 ± 6)	I	SSW	n	…	Spiral
2001 Aug 31 0138I	88 ± 3	…	I	ICME	n	…	Spiral, S
2001 Sep 14 0205S	64 ± 4	66 ± 5	C?	ICME	Y	…	Radial, N
2001 Sep 25 2025	71 ± 7	…	I	ICME	Y	…	Spiral
2001 Oct 08 1305W	81 ± 4	(55 ± 39)	C?	HPS	n	…	Spiral
2001 Oct 11 1701S	53 ± 4	(74 ± 4)	I	SSW	Y	…	Spiral
2001 Oct 21 1648S	61 ± 6	(50 ± 4)	I	SSW	Y	…	S
2001 Oct 25 0850S	84 ± 10	(30 ± 22)	I	ICME	n	…	Spiral
2001 Nov 24 0556S	87 ± 3	(56 ± 9)	I	hss?	n	…	⊥ Spiral, N
2002 Jan 10 1544A	…	(65 ± 2)	I?	hss	Y	…	W–E, S
2002 Jan 31 2127S	67 ± 18	…	I	SSW	Y	…	E–W
2002 Mar 20 1328S	80 ± 12	(50 ± 18)	I	ICME/MC	Y	n	⊥ Spiral
2002 Apr 17 1107S	62 ± 9	(90 ± 1)	I	HPS	Y	…	E–W
2002 Apr 19 0835S	76 ± 4	(67 ± 6)	I	ICME/MC	Y	…	E–W
2002 May 18 2008S	32 ± 14	(58 ± 3)	I	SSW	Y	…	Spiral
2002 May 23 1050S	72 ± 5	(84 ± 2)	I	HPS	Y	…	W–E, N
2002 Jul 19 1441A	64 ± 20	(76 ± 6)	I	ICME	Y	…	Radial
2002 Jul 25 1259A	76 ± 14	(81 ± 7)	I?	SSW	n	…	Spiral
2002 Sep 07 1636S	80 ± 8	(89 ± 4)	I	ICME	Y	…	S
2002 Nov 09 1849S	72 ± 5	(84 ± 6)	?	SSW	n	…	Spiral, N
2002 Nov 26 2150S	70 ± 1	(71 ± 3)	I	HPS	Y	…	Spiral
2003 May 09 0455A	…	(82 ± 3)	I	hss	Y	…	W–E, S
2003 May 29 1831W	72 ± 5	(87 ± 1)	I	ICME	n	…	S
2003 May 30 1600A	…	(72 ± 2)	I	ICME	Y	…	Radial, N
2003 Aug 17 1421S	…	(84 ± 2)	I	ICME	Y	…	Spiral, N
2003 Oct 26 1908S	…	(87 ± 3)	I	Sheath	n	…	Spiral
2003 Oct 28 0206S	…	(68)	I	ICME	n	0000–0215	Radial
2003 Nov 15 0550S	…	(81 ± 2)	?	hss	n	…	Spiral, N
2004 Jan 06 1951S	…	(82 ± 3)	?	hss	n	…	Spiral
2004 Jan 22 0137S	…	(89 ± 1)	I	hss	n	n	Spiral
2004 Jul 16 2155S	…	(85 ± 3)	C	HPS	n	…	W–E, S
2004 Jul 26 2249S	57 ± 8	…	I	ICME	Y	…	W–E
2004 Sep 13 2003S	…	…	I	SSW	Y	…	Spiral
2004 Nov 07 1827	58 ± 7	…	I	Sheath	Y	…	N
2004 Nov 09 0930S	54 ± 7	(30 ± 17)	I	ICME/MC	n	0945–1000	Spiral
2005 Jan 11 2000A	…	(87 ± 2)	C	HPS	n	…	Spiral
2005 Jan 21 1711S	…	(75 ± 1)	I	ICME TE?	Y	…	E–W
2005 May 15 0238S	…	(48 ± 39)	I	hss	Y	…	E–W
2005 Jun 14 1835S	…	(63 ± 10)	I	ICME?	Y	…	⊥ Spiral
2005 Jun 16 0847S	…	(73 ± 6)	I	ICME/MC	Y	…	Spiral
2005 Jul 10 0337S	…	(82 ± 3)	I	HPS	n	…	W–E
2005 Aug 01 0605A	…	(87 ± 1)	?	SSW	n	…	E–W
2005 Sep 02 1450A	…		I	SSW	Y	…	W–E, N

[a]Shock time: S, storm sudden commencement time; W, time of passage at WIND; A, time at ACE, and I, time at IMP 8. θ_{Bn} in column 2 is from the Kasper database, generally at WIND. Values of θ_{Bn} in column 3 in square brackets are WIND values from *Berdichevsky et al.* [2000], while those in parentheses are from the ACE shock list. Shock type C (I) denotes a CIR (ICME-driven) shock.

[b]Structure through which the shock is propagating at the time of observation: "HPS," heliospheric plasma sheet; "ICME," interplanetary coronal mass ejection ("/MC" indicates a magnetic cloud); "hss," high-speed stream from a coronal hole; "Sheath," sheath between an ICME and the related upstream shock; "ICME TE," at or closely following the trailing edge of an ICME.

[c]Evidence of shock-drift acceleration in ~1 MeV ions: "…," low intensity or data gap; "Y," evidence of ion intensity spike in the vicinity of shock passage. "n," observations available but feature is not evident. Times of pancake distributions observed by the IMP 8 GME are given.

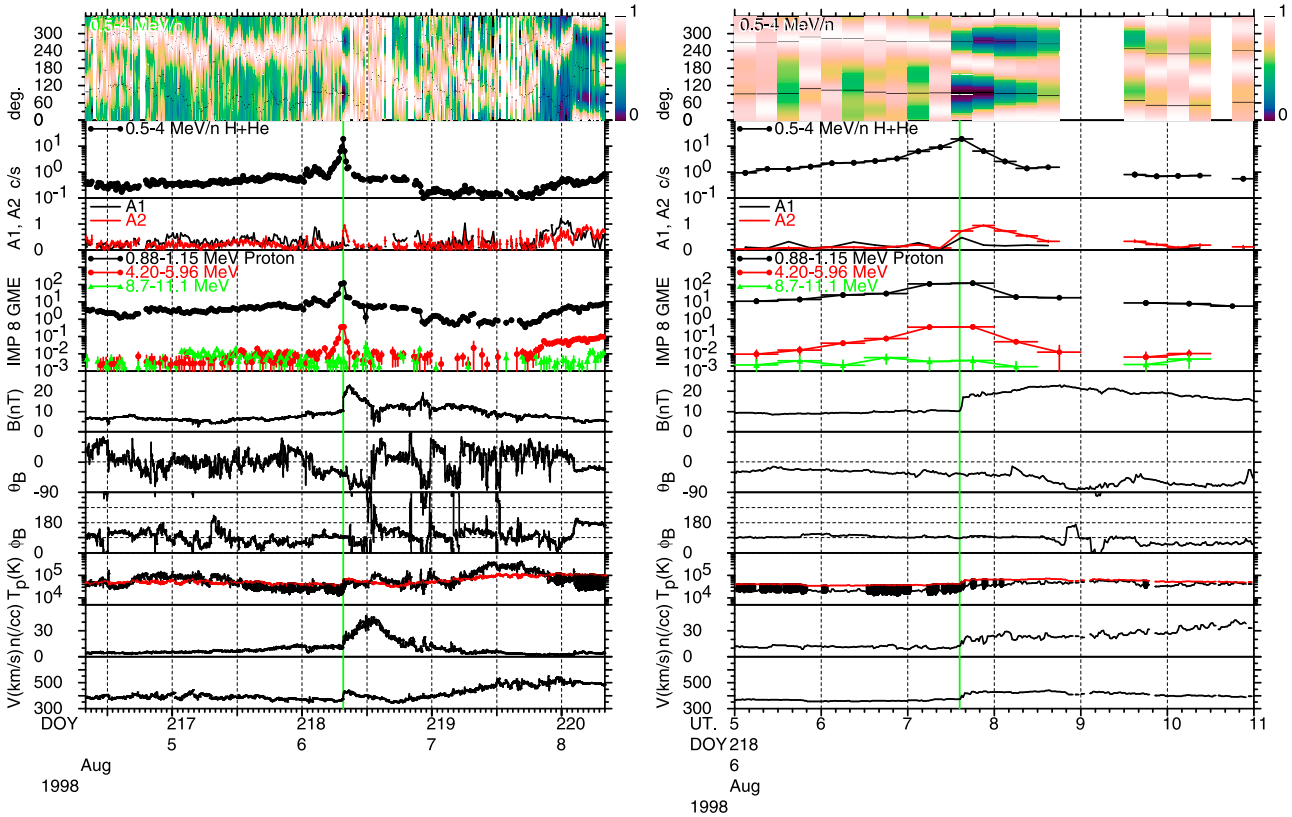

Figure 1. Energetic particle and solar wind magnetic field and plasma observations for (left) 4 days and (right) 6 hours around the passage of an interplanetary shock on August 6, 1998 (green vertical line). Particle observations are from the IMP 8 GME, and solar wind data are from the 1 minute OMNI database. Evidence of shock drift acceleration, suggestive of a quasi-perpendicular shock, includes the brief particle intensity spike at shock passage (second and fourth panels), and pancake ion distributions peaked perpendicular to the magnetic field direction commencing at shock passage (first panel).

muthal sectors as the spacecraft spins which are then transformed into the solar wind frame [*Ipavich*, 1974]. After the failure of the IMP 8 magnetometer in June 2000, we used data from the 1-minute OMNI data base (http://omniweb.gsfc.nasa.gov/) to estimate the local magnetic field direction for comparison with the particle distribution. Due to data gaps and time spent inside the Earth's bow shock, GME can only provide observations of the interplanetary particle angular distribution for a subset of the shocks in our study period. To supplement these observations, we examined ~1 MeV proton intensity-time profiles from GME, the COSTEP [*Müller-Mellin et al.*, 1995] and ERNE [*Torsti et al.*, 1995] instruments on SOHO, and the EPAM instrument on ACE [*Gold et al.*, 1998], for evidence of a spike-like increase in the particle intensity (e.g., an increase of at least a factor of two in intensity extending over a period of <~4 hours) in the vicinity of the shock.

[11] To illustrate the use of IMP 8 observations to identify a quasi-perpendicular shock, Figure 1 shows a shock that passed Earth on August 6, 1998. Two views are shown, extending over 4 days (left) and 6 hours (right) around the shock. The top plot of each panel shows the 0.5 – 4.0 MeV/n proton + He intensity as a function of viewing azimuth about the spacecraft (in GSE coordinates) resulting from a 3rd-order Fourier fit to the sectored intensities in the solar wind frame averaged over 15 minute periods [e.g., *Richardson and Reames*, 1993; *Richardson et al.*, 2008]. The intensities in a given averaging period are normalized to the maximum intensity. Thus, particle flows away from the Sun along the Parker spiral would be indicated by white/pink shading around ~315°, while Sunward flows would be indicated by similar shading at ~135°. Black horizontal line segments indicate the directions parallel and anti-parallel to the measured local magnetic field direction along which the particle flows are typically aligned, as expected. The second and third plots show the corresponding direction-averaged counting rate and the amplitudes of the first and second order Fourier components. The fourth plot shows proton intensities at 0.88 – 11.1 MeV in three GME energy channels. Below this are plots of the solar wind magnetic field intensity and polar and azimuthal angles (in GSE-coordinates), proton temperature, density and speed, in this case from the 1 minute OMNI database. Passage of the shock is indicated by the vertical green line. The proton intensity clearly shows a narrow spike that lasted for ~3 hours and peaked close to shock passage at a level around an order of magnitude higher than the ambient intensity at ~1 MeV. The spike was observed up to energies of ~6 MeV. The top panel shows that within the spike, commencing at shock passage and extending for around 2 hours, the highest intensities were found perpen-

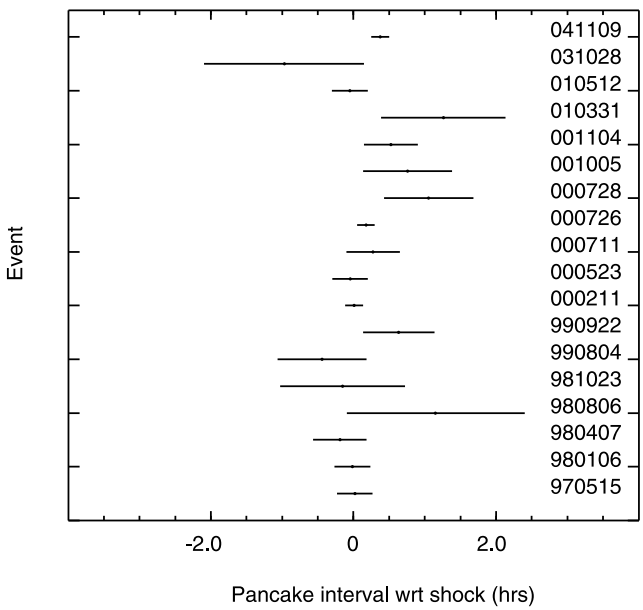

Figure 2. Times of pancake distributions observed by the IMP 8 GME with respect to shock passage (the event date is given on the right). Positive times are after shock passage.

dicular to the magnetic field and lowest along the field direction, characteristic of a pancake distribution. Consistent with such evidence of shock drift acceleration, the Kasper and ACE shock lists give θ_{Bn} = 81 ± 1° and 82 ± 3°, respectively, both indicating a nearly perpendicular shock.

3. Results

3.1. Quasi-perpendicular Shocks

[12] Of ~350 individual fast forward shocks during 1996 – October 2005 included in the Kasper, ACE or *Berdichevsky et al.* [2000] shock lists, 57 (~16%) have $\theta_{Bn} \geq 80°$ in at least one of these lists (Tables 1 and 2). Interestingly, where two estimates of θ_{Bn} are listed in Tables 1 and 2, in only 8 cases do both estimates meet our criterion to be quasi-perpendicular. Possible reasons for the differing estimates of θ_{Bn} include true differences in shock configuration at individual spacecraft [e.g., *Russell et al.*, 1983; *Szabo*, 2005] and variations in analysis methods.

[13] Considering quasi-perpendicular shocks suggested by ~1 MeV ion observations, we have identified 68 shocks that show an intensity "spike" in the vicinity of the shock, indicated by "Y" (yes) in the "spike" column in Tables 1 and 2, and 19 shocks with pancake-like particle distributions. (We note that a subset of the "energetic storm particle" events reported by *Huttunen-Heikinmaa and Valtonen* [2009] correspond to the shock spikes in our study.) The times at which pancake distributions were evident at IMP 8 are listed in the "pancake" column of Tables 1 and 2. (*Torsti et al.* [2006] reported pancake distributions at the August 11, 2000 shock and this is also indicated in Table 1.) A summary is also provided of the ~1 MeV particle features at all the shocks in Tables 1 and 2, where "n" (no) indicates that the feature was not present, "…" means that the intensity was low (close to background) in the vicinity of the shock, and "dg" denotes that there was a data gap. Around 39% (67%) of the shock spike events are associated with at least one report of $\theta_{Bn} \geq 80°$ (≥70°). Considering shocks with pancake distributions, 37% (58%) are associated with shocks reported to have $\theta_{Bn} \geq 80°$ (≥70°). Overall, all but seven shocks in Tables 1 and 2 have at least one estimate of $\theta_{Bn} > 60°$. Although there is a tendency for shocks associated with particle spikes or pancake distributions to have larger values of θ_{Bn}, the reasons for the lack of a one-to-one association between the occurrence of shock drift acceleration signatures and $\theta_{Bn} \sim 90°$, and differences between estimates of θ_{Bn} for the same shock, require further investigation which is beyond the scope of this study.

[14] Figure 2 shows the close relationship between the time of shock passage and the intervals of pancake distributions observed at IMP 8. Typically, pancake distributions commence close to shock passage and generally extend into the downstream (post-shock/positive time) region, as expected from shock drift acceleration theory, with durations of ~15 minutes to ~2.5 hours. The pancake distributions clearly demonstrate the distinct but localized effect of the shock on the ~1 MeV ion population.

[15] The October 28, 2003 shock is unusual in that the pancake distribution was observed for an extended interval (~2 hours) prior to shock passage. We also have identified even more extended intervals of pancake distributions upstream of the August 10, 1998 and January 31, 2001 shocks (in the latter case, pancake distributions persisted for ~16 hours). We have decided not to include these two shocks here because it is unclear whether these extended upstream pancake distributions are indicative of shock-drift acceleration, and hence of a quasi-perpendicular shock, or arise in some other situation. Furthermore, none of the estimates of θ_{Bn} for these shocks meet our criterion to be quasi-perpendicular.

[16] Combining the plasma/field and energetic particle identifications gives the 105 shocks in Tables 1 and 2, comprising ~30% of the 350 shocks identified in the various shock lists during the study period. The majority of these shocks (87%) were probably driven by ICMEs.

3.2. Interaction of Quasi-perpendicular Shocks With Solar Wind Structures

[17] We next consider the interplanetary circumstances that gave rise to these quasi-perpendicular shocks, in particular the types of solar wind structures through which these shocks were propagating at the time of observation. These structures are indicated in the fifth column of Tables 1 and 2.

3.2.1. Shocks Propagating Through ICMEs

[18] We first consider shocks propagating through ICMEs. Figure 3 illustrates the types of data typically considered for each shock, in this case for an ICME-driven shock observed on October 5, 2000 (second vertical green line) that was encountering a preceding, unrelated ICME. This ICME arrived in the vicinity of Earth at ~11 UT on October 3 following a shock early on this day (first vertical green line). The ICME had a magnetic cloud structure [*Klein and Burlaga*, 1982; *Lepping et al.*, 2006] including an enhanced magnetic field with a slow rotation in direction, in this case turning from northward ($\theta_B \sim 90°$) in the leading half of the ICME to southward ($\theta_B \sim -90°$) in the trailing half. Several

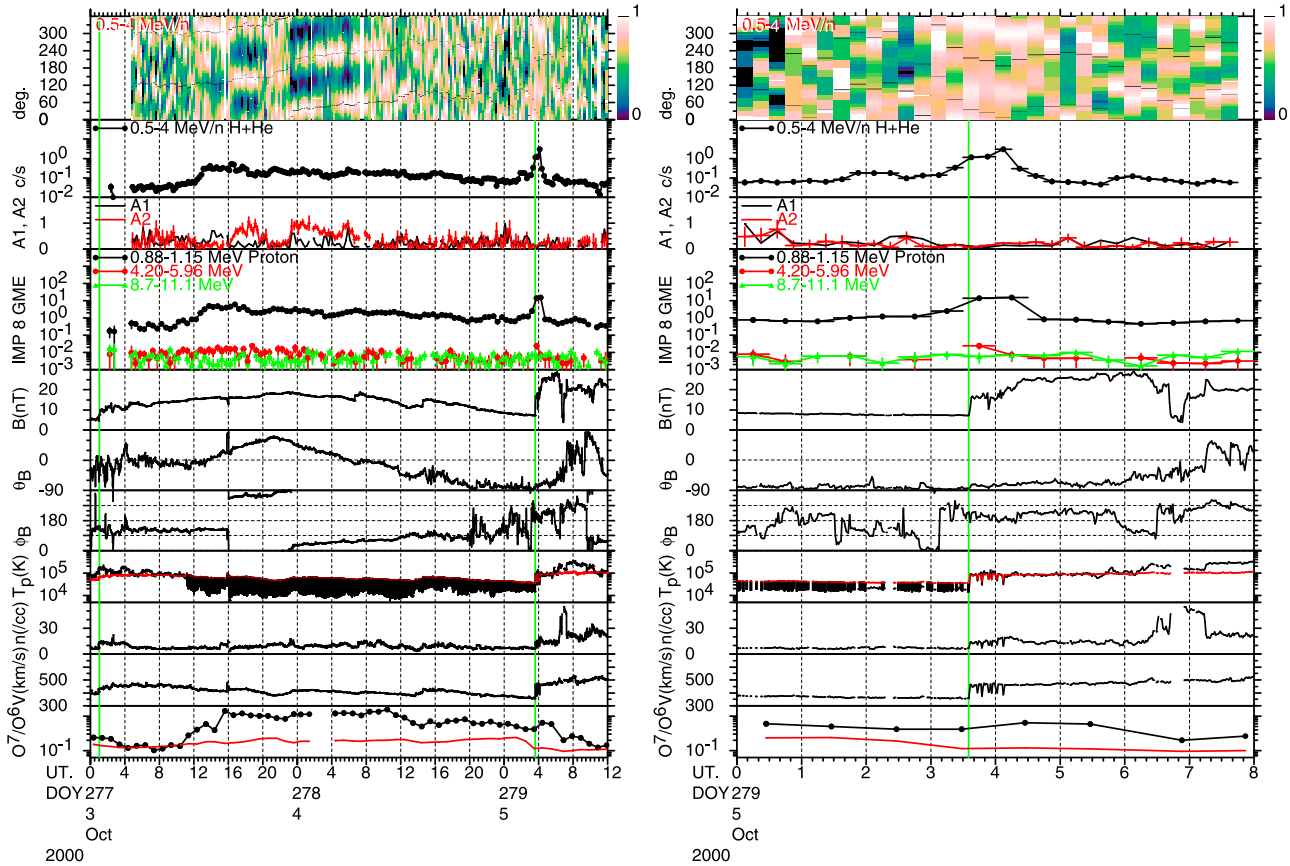

Figure 3. Energetic particle and solar wind magnetic field and plasma observations in the vicinity of an interplanetary shock on October 5, 2000 (second vertical green line) that was propagating into an ICME that arrived at ~11 UT on October 3 following a shock early on that day (first vertical green line). Particle observations are from the IMP 8 GME and solar wind data are from the 1 minute OMNI data base. The bottom panel shows the solar wind O^7/O^6 ratio measured by the SWICS instrument on ACE.

other signatures in Figure 3 support the presence of the ICME (for a summary of in-situ ICME signatures, see *Zurbuchen and Richardson* [2006]). Abnormally low solar wind proton temperatures, a frequent signature of ICMEs [e.g., *Richardson and Cane*, 1995] are indicated by black shading in the T_p panel where the condition $T_p < 0.5T_{ex}$ (T_{ex} is the "expected temperature" for normal (non-ICME) solar wind, shown by the red graph) is met. (See *Richardson and Cane* [1995] for further information on T_{ex}.) Enhanced solar wind oxygen ion charge states, as indicated by the O^7/O^6 ratio, were observed by the SWICS instrument on ACE within the ICME. Here, the red line indicates the "expected value" of O^7/O^6 in normal solar wind for comparison (see *Richardson and Cane* [2004] for further discussion). The solar energetic particle event commencing early on October 3 developed field-aligned bidirectional ion flows within the ICME which are evident as double ~horizontal stripes in the IMP 8 ion anisotropies shown in the first panel of Figure 3. Such flows are also characteristic of some ICMEs [e.g., *Marsden et al.*, 1987; *Richardson and Reames*, 1993; *Richardson and Cane*, 2008].

[19] The magnetic field was near-southward for a period of ~8 hours ahead of, and at the time of shock passage. For a radially propagating shock, this field direction would give rise to a near-perpendicular shock, although the ACE shock list indicates that the normal to this shock was in fact directed 25° from the radial direction, and the estimates of θ_{Bn} for this shock in Table 1 (74° and 66°) do not quite meet our criterion for the shock to be quasi-perpendicular. On the other hand, the IMP 8 ion observations provide evidence that the shock should be classified as quasi-perpendicular. In particular at ~1 MeV/n, there was a brief ~2 orders of magnitude intensity spike at shock passage with a duration of ~1 hour, while (though less conspicuous than in the event in Figure 1) pancake distributions commenced at the shock and extended for ~75 minutes following the shock. (Note that other than in the shock spike, the sectored count rates are too low to calculate meaningful ion distributions from 15-minute-averaged data after around midday on October 4.)

[20] Some 32 of the 105 shocks in Tables 1 and 2 (30%) were probably propagating though ICMEs. We include here cases indicated by " ICME TE" when the shock was observed closely following what may have been the trailing edge of an ICME (which is frequently ill-defined in the plasma/field data) and may still have been encountering structures associated with the ICME.

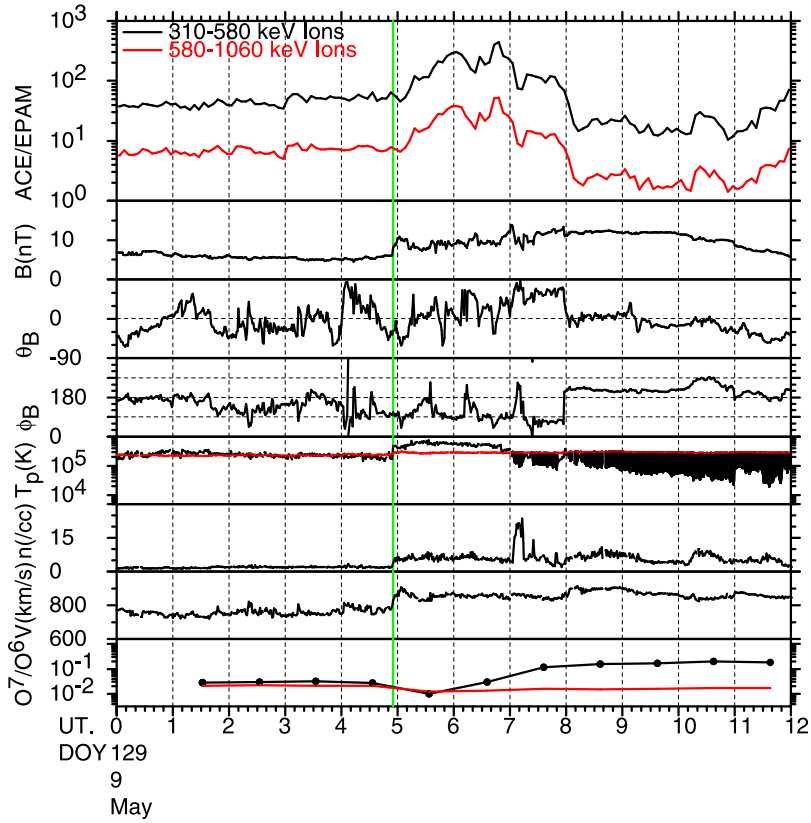

Figure 4. Energetic ion observations from the EPAM instrument on ACE, and ACE solar wind observations, in the vicinity of a quasi-perpendicular shock on May 9, 2003, that was propagating through a high-speed stream.

3.2.2. Heliospheric Plasma Sheet/Slow Solar Wind

[21] The heliospheric plasma sheet was involved in 28 (27%) of the shocks in Tables 1 and 2. We identify the HPS, associated with flows from the streamer belt, as a region of dense plasma lying around the heliospheric current sheet (HCS) that is often distinct from the compressional density enhancement associated with CIRs [e.g., *Borrini et al.*, 1981; *Gosling et al.*, 1981; *Winterhalter et al.*, 1994; *Crooker et al.*, 2004].

[22] To understand how the HPS might contribute to quasi-perpendicular shock configurations, we note that *Behannon et al.* [1981] reported that crossings of the HCS may be complex, including non-spiral fields and discontinuities tilted at large angles to the ecliptic, while *Lepping et al.* [1996] and *Blanco et al.* [2008] have discussed how the HCS may be highly inclined to the ecliptic. A transient component in the HPS has also been discussed [e.g., *Crooker et al.*, 1996, 2004]. Evidently, field deviations do occur in the vicinity of the HCS/HPS and may help to account for the frequent formation of quasi-perpendicular shocks propagating through the HPS. Another 26 shocks in Tables 1 and 2 (25%) were propagating through the slow solar wind (SSW) but the HPS did not appear to be present in the vicinity of the shock.

3.2.3. High-Speed Streams

[23] Twelve shocks in Tables 1 and 2 (11%) were propagating through high-speed solar wind streams (hss) that originated in coronal holes. One such event, the ICME-driven shock of May 9, 2003 (θ_{Bn} = 82° at ACE), is shown in Figure 4. This shock was propagating through solar wind with speeds of ~750 km/s associated with a corotating high speed stream that persisted from October 2002 to January 2004. We show this event since it illustrates how the quasi-perpendicular nature of a shock may be determined by the magnetic field orientation at the shock in a region of variable field direction, in this case associated with large amplitude Alfvén waves propagating away from the Sun, a typical feature of corotating high-speed streams [e.g., *Belcher and Davis*, 1971]. The anti-correlated variations in the individual components of the solar wind velocity and magnetic field direction immediately upstream of the shock in Figure 5 indicate the presence of Alfvén waves. In particular, the field was directed west to east ($B_x \sim 0$; $\phi_B \sim 90°$) and southward at shock passage. Combined with the closely radially propagating shock (the normal was only 4° from the radial direction), a quasi-perpendicular shock configuration was the result. However, this configuration is unlikely to have been maintained as the shock moved out through the Alfvén wave field. The ~1 MeV ion data from ACE/EPAM in Figure 6 show an enhancement that does not encompass the shock, but extends for ~3 hours following the shock, until the arrival of the ICME driving the shock, at ~8 UT.

3.2.4. Sheath

[24] We finally identify 7 shocks (7% of the shocks in Tables 1 and 2) that were probably observed within the sheath

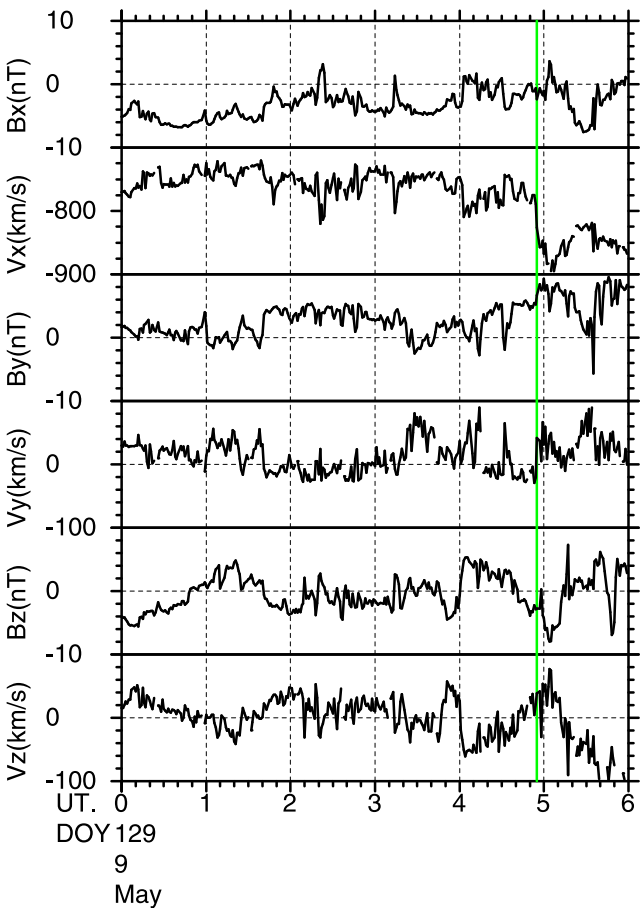

Figure 5. Magnetic field and solar wind velocity components (in GSE coordinates) at ACE in the vicinity of the shock illustrated in Figure 4. Anti-correlations between the field and velocity components indicate that the shock (vertical green line) was propagating through Alfvén waves moving away from the Sun.

of an unrelated shock, i.e., in the region of compressed, heated plasma lying between the unrelated shock and driving ICME. We might expect some quasi-perpendicular shocks to be observed within sheaths because of the substantial field direction variations that may be present, including field draping around the ICME [e.g., *McComas et al.*, 1988, 1989; *Liu et al.*, 2008], and the possibility that at times of high activity, shocks will be found propagating through the sheaths of preceding shocks. Evidently however, this situation only accounts for a small fraction of our sample of quasi-perpendicular shocks.

3.3. What Factors Determine the Type of Structures Encountered by Quasi-perpendicular Shocks?

[25] Figure 6 summarizes the solar wind structures upstream of all the shocks in Tables 1 and 2 and for sub groups defined by $\theta_{Bn} \geq 80°$, ion pancake distributions, or shock spikes. With the exception of the group of shocks defined by pancake distributions, overall around a third of the shocks were propagating into an ICME. Another ~quarter were propagating through the HPS, and a further ~quarter through slow solar wind away from the HPS. Around 10% were propagating through high-speed streams and about one in fifteen was observed in the sheath of another shock.

[26] Considering shocks defined by pancake ion distributions, 58% of these shocks were propagating through ICMEs, another quarter through the HPS, and relatively few through other slow or fast solar wind (6% in each case). The differences from the results summarized in the preceding paragraph may arise from the smaller sample size, or, more interestingly, it is possible that the slowly varying field directions often found in ICMEs and present at the times of several of these shocks (e.g., the events in Figures 1 and 3) may allow the quasi-perpendicular configuration to persist for longer intervals and favor the development of clear pancake distributions in the vicinity of the shock. This aspect could be examined further by using the extensive IMP 8 GME database since 1973 to identify a larger sample of shocks associated with pancake distributions, but such a study is beyond the scope of this paper.

[27] Figure 7 examines how the occurrence rates of quasi-perpendicular shocks and the structures upstream of quasi-perpendicular shocks, and within the solar wind as a whole, vary through our study period. The top panel shows the monthly sunspot number to indicate the progress of solar cycle 23. The second panel shows the yearly occurrence rate

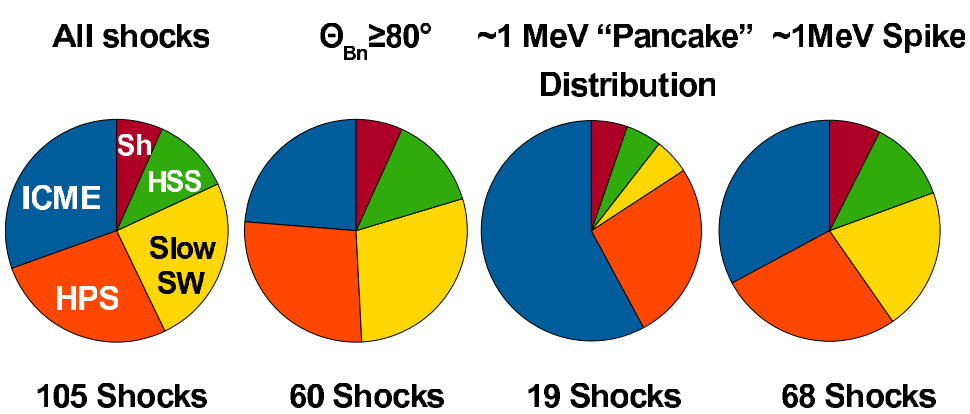

Figure 6. Summary of the solar wind structures upstream of all the shocks in this study and subsets defined by $\theta_{Bn} \geq 80°$, and the presence of ~1 MeV pancake distributions and shock spikes.

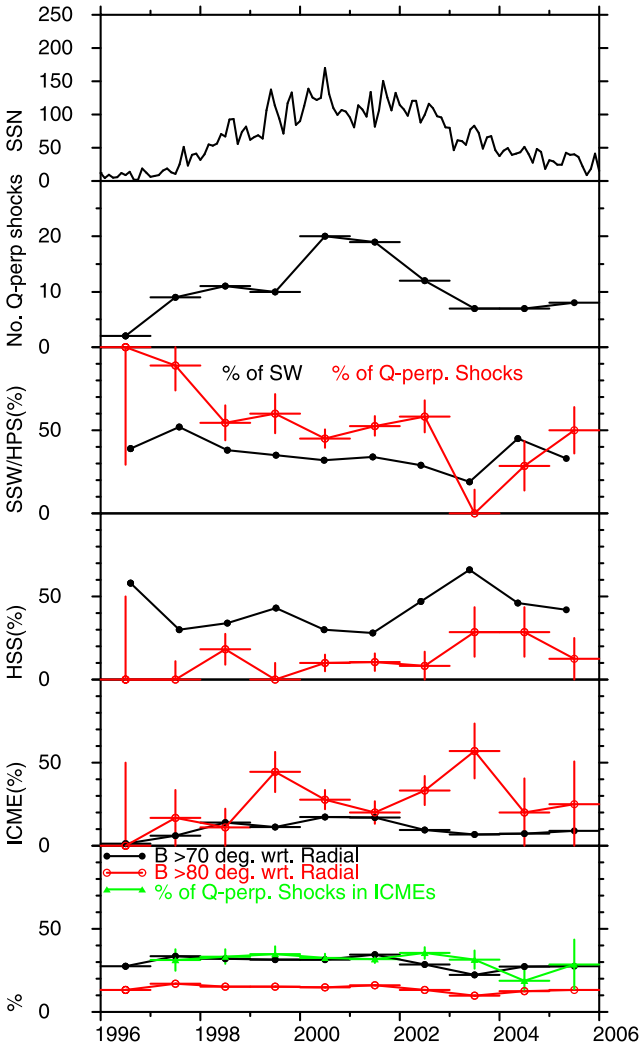

Figure 7. Comparison of the percentage of the near-Earth solar wind occupied by slow solar wind (third panel, black graph), high-speed streams (fourth panel, black graph), and ICMEs (fifth panel, black graph) with the percentage of the quasi-perpendicular shocks that were propagating through these structures (red graphs) during 1996–2005. For comparison with the slow solar wind fraction, the shocks propagating into slow solar wind and the heliospheric plasma sheet are combined. The first panel shows the monthly sunspot number, while the second panel gives the number of shocks in each year in Tables 1 and 2. The sixth compares the percentage of the time when the solar wind magnetic field is directed ≥70° and ≥80° from the radial direction (black and red graphs, respectively), while the green graph indicates the fraction of all identified shocks that are quasi-perpendicular based on plasma/field and energetic particle observations.

of the shocks in Tables 1 and 2. This largely follows solar activity levels, as expected since ~90% of the shocks were probably associated with ICMEs and the ICME rate tends to follow solar activity levels [e.g., *Cane and Richardson*, 2003; *Richardson and Cane*, 2010].

[28] We might expect the occurrence rates of the different types of upstream structures to be determined to a large extent by the fraction of the near-Earth solar wind occupied by each type of structure. To examine this, the black graphs in the third and fourth panels of Figure 7 show, respectively, the percentage of the time that the near-Earth solar wind was occupied by slow solar wind (SSW) or high speed streams from coronal holes (HSS), averaged over intervals of 13 solar (Carrington) rotations (~1 year). These percentages are updated from the analysis of solar wind plasma and field data described by *Richardson et al.* [2000, 2002] [see also *Emery et al.*, 2009]. The solar wind structure list is available at http://cedarweb.hao.ucar.edu/wiki/index.php/Tools_and_Models:Solar_Wind_Structures. The black graph in the fifth panel shows the percentage of time when the solar wind was occupied by ICMEs included on our ICME list. This also follows the solar cycle.

[29] Figure 7 also shows how the percentages of quasi-perpendicular shocks propagating through different types of upstream structures vary with time. Since in the solar wind classification we have not attempted to separate the HPS from other slow solar wind, in the third panel we show in red the percentage of quasi-perpendicular shocks propagating through either the HPS or slow solar wind in each year. The "error bars" indicate how the percentages would vary if the number of shocks were changed by ±1. The percentage of quasi-perpendicular shocks propagating through high-speed streams is similarly plotted in red in panel 4, while the percentage of quasi-perpendicular shocks propagating through ICMEs is shown in red in panel 5.

[30] In general, the percentage of quasi-perpendicular shocks propagating through slow solar wind is around a half as large again as the percentage of solar wind occupied by slow solar wind (e.g., typically ~60% compared with ~40%), at least until the decay phase of the solar cycle. This result suggests that quasi-perpendicular shocks are found in the slow solar wind more frequently than might be expected based on the fraction of the solar wind occupied by slow solar wind. Note also that both of the shocks in 1996 were CIR forward shocks propagating into slow solar wind or the HPS.

[31] The percentage of shocks propagating through high-speed streams (panel 4) is substantially lower than might be expected based on the time when high-speed streams were present (typically ~10% compared with ~30%, i.e., ~one third of the expected rate). Possible contributing factors may include the general absence of solar active regions within the coronal holes that produce high-speed streams, the reduced pitch of the Parker spiral within high-speed streams, the higher ICME speeds necessary to drive shocks in high-speed solar wind, and the presence of Alfvén waves within high-speed streams. In addition, for CIR-associated shocks, we only consider forward shocks that are propagating into slow solar wind, though such shocks only form a minority of our sample.

[32] The percentage of shocks propagating through ICMEs (panel 5) is comparable or larger than the percentage of the solar wind occupied by ICMEs. As noted above around a third of quasi-perpendicular shocks were propagating through ICMEs. Since the fraction of solar wind occupied by ICMEs was ~10% during the study period and

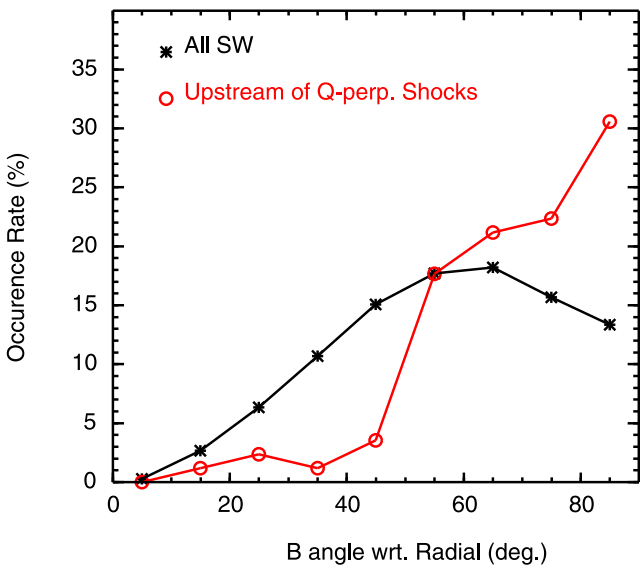

Figure 8. Occurrence rates of the angle between the radial direction and the magnetic field direction upstream of 85 quasi-perpendicular shocks (red) and in all the solar wind during the study period (black).

~15% at solar maximum when the shock rate was highest, this suggests that quasi-perpendicular shocks were found inside ICMEs around 2–3 times more frequently than would be expected. The unusually high percentages in 1999 and 2003 may have been enhanced by the absence of shocks moving through high-speed streams and slow solar wind, respectively. Note that the 2003 enhancement is not simply due to shocks associated with the "Halloween" solar events in late October-early November; shocks earlier in the year also contribute (see Table 2).

3.4. Magnetic Field Direction Upstream of Quasi-perpendicular Shocks

[33] We have also examined the direction of the magnetic field upstream of the shocks in Tables 1 and 2, based on 1-minute averaged field data. First, we have summarized this direction for each shock in the right-hand column of Tables 1 and 2. The field azimuth is assigned to eight 45° width bins centered on: the inward or outward radial directions (ϕ_B (in GSE coordinates) = 0° or 180°), the west-east or east-west directions (ϕ_B = 90° or 270°), outward and inward Parker spiral directions (ϕ_B = 135° or 315°), and inward and outward directions perpendicular to the Parker spiral (ϕ_B = 45° or 225°). If the field was inclined between 35° and 65° north or south of the ecliptic, this is also noted in addition to the azimuthal direction. If the field was inclined ≥65° from the ecliptic, the direction is summarized as either north (N) or south (S) as appropriate. The most common circumstance is for the magnetic field azimuth to be directed ~perpendicular to the radial direction. In particular, the field was east to west or west to east ahead of 45 shocks (43% of 105 shocks), and was strongly northward or southward ahead of 13 shocks. Together, these account for 55% of the shocks in Tables 1 and 2. Another 33 shocks (31%) had spiral upstream fields, 6 shocks (6%) had radial fields (an unlikely direction for the field upstream of a radially propagating quasi-perpendicular shock) and for 8 shocks (8%) the upstream magnetic field was perpendicular to the Parker spiral, the low number of such shocks presumably reflecting the low occurrence rate (~10%) of such field orientations in the solar wind.

[34] Figure 8 compares the occurrence rates (in 10° bins) of the angle between the radial and magnetic field directions immediately upstream of 85 ICME-driven quasi-perpendicular shocks (red graph), and in all the solar wind during the study period (black graph). The field upstream of these shocks is clearly more likely to be inclined at angles >60° to the radial direction than in average solar wind, while smaller angles are rarer, as would be expected assuming that these shocks are typically propagating ~radially away from the Sun. In particular the magnetic field is 2.3 times more likely to lie 80 – 90° from the radial direction upstream of these shocks.

[35] Since magnetic field orientations approximately perpendicular to the outward radial direction may favor the formation of quasi-perpendicular ICME-driven shocks (assuming that these shocks are propagating ~radially away from the Sun), we have also investigated the occurrence of such field orientations in the solar wind at 1 AU. The sixth panel of Figure 7 shows the percentages of time when the field was directed ≥70° (black; ~30%) and ≥80° (red; ~15%) from the radial direction. (Note there is little variation with solar activity levels.) The percentage of all the ICME-driven shocks in our study period that are quasi-perpendicular based on plasma/field or particle observations is indicated in green. Overall, the fraction of quasi-perpendicular shocks is similar to the fraction of the time when the solar wind is oriented at large angles (>70°) to the radial direction, suggesting that the orientation of the interplanetary magnetic field may help to determine the shock configuration.

[36] It would be interesting to examine the distribution of values of θ_{Bn} for shocks propagating through different types of solar wind structure and hence assess the influence of solar wind structure type on θ_{Bn}. However, such a study would require the upstream solar wind structures to be identified for a larger sample of shocks with a range of values of θ_{Bn} which is beyond the scope of the present paper. We can however examine how values of θ_{Bn} compare for shocks propagating into ICMEs and those observed outside ICMEs since we have already compiled a comprehensive list of ICMEs for cycle 23, as described in section 2. One complication, as noted above, is that independent estimates of θ_{Bn} can differ significantly. Thus in Figure 9, we combine estimates of θ_{Bn} from the Kasper data base, plotted on the vertical axis, with those from the ACE shock list or *Berdichevsky et al.* [2000] (plotted on the horizontal axis) for 176 shocks for which two estimates of θ_{Bn} are available (error bars, which can be substantial, are not shown). The bottom panel shows results for 39 shocks propagating into ICMEs, while the top panel shows 137 other shocks not propagating into ICMEs. Our general conclusion is that shocks propagating into ICMEs tend to have larger values of θ_{Bn} than other shocks. In particular, 69% of the shocks propagating into ICMEs have both estimates of $\theta_{Bn} \geq 50°$ compared with 43% for the other shocks. To investigate why shocks observed inside ICMEs may have larger values

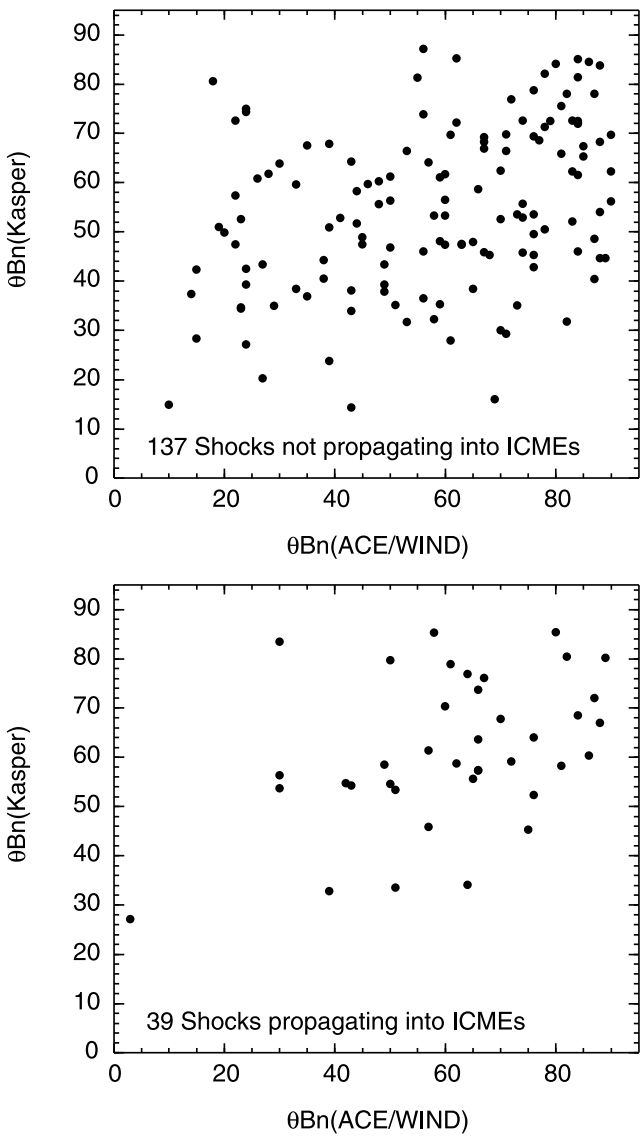

Figure 9. θ_{Bn} from the Kasper database plotted against θ_{Bn} from the ACE shock list or *Berdichevsky et al.* [2000] (bottom) for shocks propagating into ICMEs and (top) for other shocks.

of θ_{Bn}, Figure 10 shows the occurrence rate of the angle between the radial and IMF directions (~θ_{Bn} for a radially propagating shock) in 10°-width bins relative to the occurrence rate in all solar wind (black graph in Figure 8) for magnetic fields within ICMEs during the study period that are, or are not, magnetic clouds. Values above 1 indicate that the field was more likely to lie in a given range than in the solar wind as a whole. The results show that angles above ~70° are ~30% more likely to occur in magnetic clouds whereas their occurrence rate is only slightly enhanced in other ICMEs. In addition, intermediate angles are less likely to be found inside ICMEs. Thus, in particular in magnetic clouds, the magnetic fields in ICMEs may be more conducive for the production of quasi-perpendicular shock configurations than in the solar wind as a whole. Note also that small field angles with respect to the radial tend to be found more frequently in ICMEs, though the occurrence rates are still low compared to higher angles.

4. Summary

[37] We have examined the interplanetary circumstances of 105 near-Earth quasi-perpendicular fast forward shocks in 1996–2005 identified either using estimates of θ_{Bn} with a criterion of $\theta_{Bn} \geq 80°$, or by evidence of shock drift acceleration in observations of ~1 MeV ions. Our major conclusions are:

[38] 1. Around 87% of these shocks were probably generated by ICMEs, the remainder by CIRs. Together, these shocks represent ~30% of all the shocks identified at 1 AU during the study period.

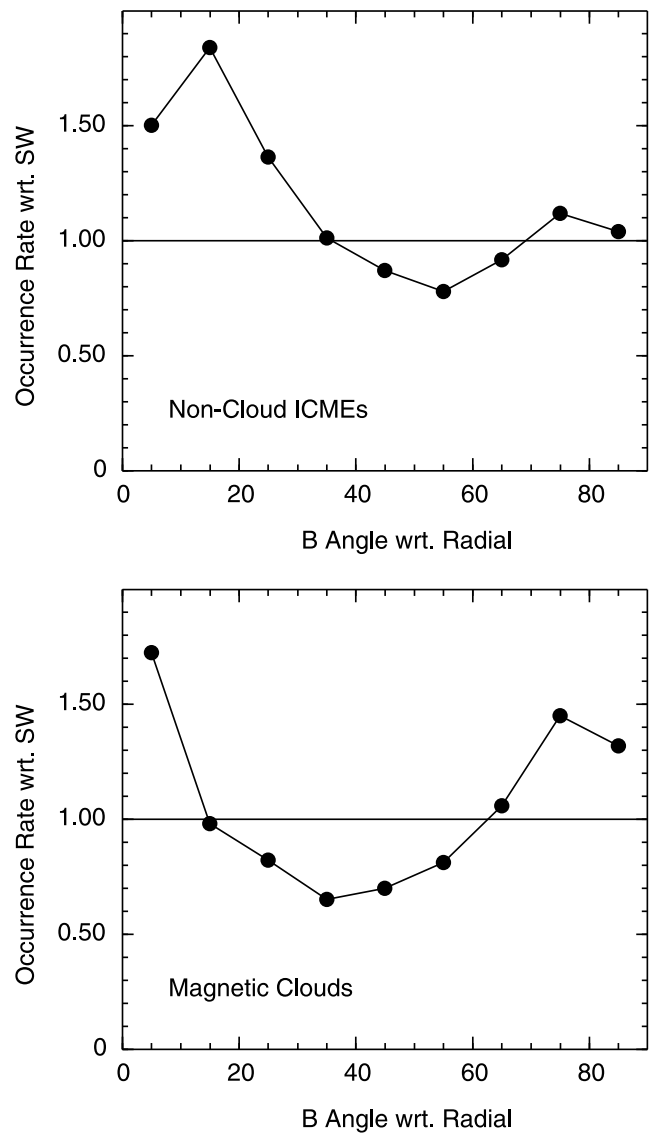

Figure 10. Ratio of the probability of the angle between the magnetic field and radial directions inside ICMEs that are or are not magnetic clouds lying in 10° bins compared with the solar wind as a whole (black graph in Figure 8).

[39] 2. These shocks were propagating into a variety of solar wind structures including ICMEs, accounting for around a third of the shocks, and the heliospheric plasma sheet and other slow solar wind, each accounting for around a quarter of the events. Around 11% were observed in a high-speed stream, and 7% in the sheath following a previous shock.

[40] 3. The association rates with each type of structure varied during solar cycle 23. Quasi-perpendicular shocks were observed more frequently propagating through slow solar wind than would be expected based on the fraction of the solar wind occupied by slow solar wind whereas the occurrence rate in high-speed streams was only around a third of that expected. The fraction of shocks propagating through ICMEs was around 2–3 times larger than expected, suggesting a preference for quasi-perpendicular shocks to be found propagating through ICMEs.

[41] 4. Magnetic fields upstream of ICME-driven quasi-perpendicular shocks are more likely to be inclined at large angles to the radial direction than is found generally in the solar wind, with the most probable angle being >80°. Such a field orientation combined with a radially directed shock would give rise to a quasi-perpendicular shock configuration. The fraction of fast forward shocks that are quasi-perpendicular is similar to the fraction of the time when the solar wind is at large angles (>70°) to the radial direction.

[42] 5. The formation of pancake ion distributions may be favored at shocks propagating through ICMEs, although a larger sample of shocks should be examined to confirm this. A possible reason is that the smoothly varying field direction in some ICMEs, in particular magnetic clouds (such as in Figure 3) may allow the quasi-perpendicular configuration to be maintained for a longer period, allowing clear signatures of shock-drift acceleration to develop. However, it is difficult to evaluate the relationship between the level of magnetic field variations and the presence of pancake distributions because it is the past history of the magnetic field, contained in the downstream region and distorted by the passage of the shock, that is most relevant, not the future development as determined by the upstream conditions.

[43] 6. Shocks propagating through ICMEs tend to have larger values of θ_{Bn} than other shocks. In particular, 69% of shocks with two estimates of θ_{Bn} from the Kasper and another shock list had both estimates >50° compared to 43% for other shocks. The higher occurrence rates of magnetic fields highly inclined to the radial direction, in particular in magnetic clouds, and lower occurrence of "intermediate" orientations, may contribute.

[44] 7. It is probably unrealistic in studies of particle acceleration by shocks to regard a local estimate of θ_{Bn} as an indicator of the "global" shock configuration. For example, as noted above, there is frequently a lack of agreement between the values of θ_{Bn} derived from data from different near-Earth spacecraft or by different researchers (see Figure 9). Energetic particle data do not always help to confirm the shock configuration - shock-drift acceleration may occur where θ_{Bn} is not consistent with a quasi-perpendicular shock, and there are quasi-perpendicular shocks that lack clear signatures of shock drift acceleration. Even in the simplest Parker spiral field, θ_{Bn} will evolve with heliocentric distance. Such factors may be problematical in studies attempting to relate event-averaged particle properties, e.g., spectra, with the deceptively simple parameter "θ_{Bn}."

[45] **Acknowledgments.** We thank Justin Kasper and Chuck Smith and co-workers for making available their shock parameter lists. The ACE data sets used in this study were provided by the ACE Science Center (http://www.srl.caltech.edu/ACE/ASC/). The SOHO COSTEP data were provided by the SOHO Data Archive (http://sohowww.nascom.nasa.gov/) while the ERNE data were obtained from the Space Research Laboratory, University of Turku (http://www.srl.utu.fi/). We acknowledge the use of data from the OMNI solar wind data base, compiled by the Space Physics Data Facility at the Goddard Space Flight Center (http://omniweb.gsfc.nasa.gov/). This work was supported by a NASA Living With a Star Targeted Research and Technology grant.

[46] Philippa Browning thanks Charles Smith and another reviewer for their assistance in evaluating this paper.

References

Armstrong, T. P., M. E. Pesses, and R. B. Decker (1985), Shock drift acceleration, in *Collisionless Shocks in the Heliosphere: Reviews of Current Research*, *Geophys. Mongro. Ser.*, vol. 35, edited by B. T. Tsurutani and R. G. Stone, p. 271, AGU, Washington, D. C.

Behannon, K. W., F. M. Neubauer, and H. Barnstorf (1981), Finescale characteristics of interplanetary sector boundaries, *J. Geophys. Res.*, *86*, 3273.

Belcher, J. W., and L. Davis (1971), Large amplitude Alfvén waves in the interplanetary medium: 2, *J. Geophys. Res.*, *76*, 3534.

Berdichevsky, D. B., A. Szabo, R. P. Lepping, A. F. Viñas, and F. Mariani (2000), Interplanetary fast shocks and associated drivers observed through the 23rd solar minimum by Wind over its first 2.5 years, *J. Geophys. Res.*, *105*, 27,289.

Blanco, J. J., J. Rodriguez-Pacheco, M. A. Hidalgo, and J. Sequeiro (2008), Monitoring the heliospheric current sheet local structure for the years 1995 to 2001, *J. Atmosph. Sol. Terr. Phys.*, *70*, 226, doi:10.1016/j.jastp.2007.08.030.

Borrini, G., J. T. Gosling, S. J. Bame, W. C. Feldman, and J. M. Wilcox (1981), Solar wind helium and hydrogen structure near the heliospheric current sheet—A signal of coronal streamers at 1 AU, *J. Geophys. Res.*, *86*, 4,565.

Borrini, G., J. T. Gosling, S. J. Bame, and W. C. Feldman (1982), An analysis of shock wave disturbances observed at 1 AU from 1971 through 1978, *J. Geophys. Res.*, *87*, 4365.

Cane, H. V. (1988), The large-scale structure of flare-associated interplanetary shocks, *J. Geophys. Res.*, *93*, 1.

Cane, H. V., and I. G. Richardson (2003), Interplanetary coronal mass ejections in the near-Earth solar wind during 1996–2002, *J. Geophys. Res.*, *108*(A4), 1156, doi:10.1029/2002JA009817.

Crooker, N. U., M. E. Burton, J. L. Phillips, E. J. Smith, and A. Balogh (1996), Heliospheric plasma sheets as small-scale transients, *J. Geophys. Res.*, *101*, 2467.

Crooker, N. U., C.-L. Huang, S. M. Lamassa, D. E. Larson, S. W. Kahler, and H. E. Spence (2004), Heliospheric plasma sheets, *J. Geophys. Res.*, *109*, A03107, doi:10.1029/2003JA010170.

Decker, R. B. (1983), Formation of shock-spike events at quasi-perpendicular shocks, *J. Geophys. Res.*, *88*, 9959.

Decker, R. B. (1990), Particle acceleration at shocks with surface ripples, *J. Geophys. Res.*, *95*(A8), 11,993.

Decker, R. B. (1993), The role of magnetic loops in particle acceleration at nearly perpendicular shocks, *J. Geophys. Res.*, *98*, 33.

Emery, B. A., I. G. Richardson, D. S. Evans, and F. J. Rich (2009), Solar wind structure sources and periodicities of auroral electron power over three solar cycles, *J. Atmos. Sol. Terr. Phys.*, *71*, 1157, doi:10.1016/j.jastp.2008.08.005.

Erdös, G., and A. Balogh (1993), Acceleration of protons trapped upstream of interplanetary shocks, *J. Geophys. Res.*, *98*, 13,253.

Erdös, G., and A. Balogh (1994), Drift acceleration at interplanetary shocks, *Astrophys. J.*, *90*, 553.

Forman, M. A., and G. M. Webb (1985), Acceleration of energetic particles, in *Collisionless Shocks in the Heliosphere: Reviews of Current Research*, *Geophys. Mongro. Ser.*, vol. 35, edited by B. T. Tsurutani and R. G. Stone, p. 91, AGU, Washington, D. C.

Gold, R. E., et al. (1998), Electron, proton and alpha monitor on the Advanced Composition Explorer spacecraft, *Space Sci. Rev.*, *86*, 541.

Gosling, J. T., G. Borrini, J. R. Asbridge, S. J. Bame, W. C. Feldman, and R. F. Hansen (1981), Coronal streamers in the solar wind at 1 AU, *J. Geophys. Res.*, *86*, 5438.

Hundhausen, A. J. (1972), Interplanetary shock waves and the structure of solar wind disturbances, in *Solar Wind*, edited by C. P. Sonett, P. J. Coleman Jr., and J. M. Wilcox, *NASA Spec. Publ.*, *NASA SP-308*, 393.

Huttunen-Heikinmaa, K., and E. Valtonen (2009), Interplanetary fast forward shocks and energetic storm particle events above 1.5 MeV, *Ann. Geophys.*, *27*, 767.

Ipavich, F. M. (1974), The Compton-Getting effect for low energy particles, *Geophys. Res. Lett.*, *1*, 149.

Klein, L. W., and L. F. Burlaga (1982), Interplanetary magnetic clouds at 1 AU, *J. Geophys. Res.*, *87*, 613.

Lee, M. A. (1983), Coupled hydromagnetic wave excitation and ion acceleration at interplanetary traveling shocks, *J. Geophys. Res.*, *88*, 6109.

Lepping, R. P., A. Szabo, M. Peredo, and J. T. Hoeksema (1996), Large-scale properties and solar connection of the heliospheric current and plasma sheets: WIND observations, *Geophys. Res. Lett.*, *23*, 1199.

Lepping, R. P., D. B. Berdichevsky, C.-C. Wu, A. Szabo, T. Narock, F. Mariani, A. J. Lazarus, and A. J. Quivers (2006), A summary of WIND magnetic clouds for years 1995–2003: Model-fitted parameters, associated errors and classifications, *Ann. Geophys.*, *24*, 215.

Liu, Y., W. B. Manchester IV, J. D. Richardson, J. G. Luhmann, R. P. Lin, and S. D. Bale (2008), Deflection flows ahead of ICMEs as an indicator of curvature and geoeffectiveness, *J. Geophys. Res.*, *113*, A00B03, doi:10.1029/2007JA012996.

Marhavilas, P. K., E. T. Sarris, G. C. Anagnostopoulos, and P. C. Trochoutsos (2003), Distinct shock acceleration processes—Evaluation of the magnetic trap dimensions formed upstream of an interplanetary shock using measurements of the Ulysses spacecraft, *Adv. Space Res.*, *32*(4), 525, doi:10.l016/SO273-1177(03)00353-3.

Marsden, R. G., T. R. Sanderson, C. Tranquille, K.-P. Wenzel, and E. J. Smith (1987), ISEE 3 observations of low-energy proton bidirectional events and their relationship to isolated interplanetary structures, *J. Geophys. Res.*, *92*, 11,009.

McComas, D. J., J. T. Gosling, D. Winterhalter, and E. J. Smith (1988), Interplanetary magnetic field draping about fast coronal mass ejecta in the outer heliosphere, *J. Geophys. Res.*, *93*, 2519.

McComas, D. J., J. T. Gosling, S. J. Bame, E. J. Smith, and H. V. Cane (1989), A test of magnetic field draping induced B_z perturbations ahead of fast coronal mass ejecta, *J. Geophys. Res.*, *94*, 1465.

McGuire, R. E., T. T. von Rosenvinge, and F. B. McDonald (1986), The composition of solar energetic particles, *Astrophys. J.*, *301*, 938.

Müller-Mellin, R., et al. (1995), COSTEP—Comprehensive Suprathermal And Energetic Particle Analyser, *Sol. Phys. 162*, 483.

Neugebauer, M., and J. Giacalone (2005), Multispacecraft observations of interplanetary shocks: Nonplanarity and energetic particles, *J. Geophys. Res.*, *110*, A12106, doi:10.1029/2005JA011380.

Parker, E. N. (1958), Dynamics of the interplanetary gas and magnetic fields, *Astrophys. J.*, *128*, 664.

Richardson, I. G. (2004), Energetic particles and corotating interaction regions in the solar wind, *Space Sci. Rev.*, *111*, 267.

Richardson, I. G., and H. V. Cane (1993), Signatures of shock drivers in the solar wind and their dependence on the solar source location, *J. Geophys. Res.*, *98*, 15,295.

Richardson, I. G., and H. V. Cane (1995), Regions of abnormally low proton temperature in the solar wind (1965–1991) and their association with ejecta, *J. Geophys. Res.*, *100*, 23,397.

Richardson, I. G. and H. V. Cane (2004), Identification of interplanetary coronal mass ejections at 1 AU using multiple solar wind composition anomalies, *J. Geophys. Res.*, *109*, A09104, doi:10.1029/2004JA010598.

Richardson, I. G., and H. V. Cane (2008), Interplanetary coronal mass ejections during 1996–2007, in *Proceedings of the 30th International Cosmic Ray Conference*, vol. 1, p. 319, Univ. Nac. Autonoma de Mexcio, Mexico City.

Richardson, I. G., and H. V. Cane (2010), Interplanetary coronal mass ejections during solar cycle 23, in *Twelfth International Solar Wind Conference*, edited by M. Maksimovic et al., *AIP Conf. Proc.*, *1216*, 683–686, doi:10.1063/1.3395959.

Richardson, I. G., and D. V. Reames (1993), Bidirectional ~1 MeV/amu ion intervals in 1973–1991 observed by the Goddard Space Flight Center instruments on IMP 8 and ISEE 3/ICE, *Astrophys. J. Suppl.*, *85*, 411.

Richardson, I. G., E. W. Cliver, and H. V. Cane (2000), Sources of geomagnetic activity over the solar cycle: Relative importance of CMEs, high-speed streams, and slow solar wind, *J. Geophys. Res.*, *105*, 18,203.

Richardson, I. G., H. V. Cane, and E. W. Cliver (2002), Sources of geomagnetic activity during nearly three solar cycles (1972–2000), *J. Geophys. Res.*, *107*(A8), 1187, doi:10.1029/2001JA000504.

Richardson, I. G., H. V. Cane, T. T. von Rosenvinge, and R. E. McGuire (2008), IMP 8 GME energetic particle observations over three solar cycles, in *Proceedings of the 30th International Cosmic Ray Conference*, vol. 1, p. 323, Univ. Nac. Autonoma de Mexcio, Mexico City.

Russell, C. T., M. M. Mellott, E. J. Smith, and J. H. King (1983), Multiple spacecraft observations of interplanetary shocks: Four spacecraft determination of shock normals, *J. Geophys. Res.*, *88*, 4739.

Sarris, E. T., and S. M. Krimigis (1985), Quasi-perpendicular shock acceleration of ions to ~200 MeV and electrons to 2 MeV observed by Voyager 2, *Astrophys. J.*, *298*, 676.

Sarris, E. T., and J. A. Van Allen (1974), Effects of interplanetary shock waves on energetic particles, *J. Geophys. Res.*, *79*, 4157.

Sarris, E. T., S. M. Krimigis, and T. P. Armstrong (1976), Observations of a high-energy ion shock spike in interplanetary space, *Geophys. Res. Lett.*, *3*, 133.

Schwenn, R. (1990), Large-scale structure of the interplanetary medium, in *Physics of the Inner Heliosphere*, vol. 1, edited by R. Schwenn and E. Marsch, p. 99, Springer-Verlag, Berlin.

Smith, E. J., and J. H. Wolfe (1976), Observations of interaction regions and co-rotating shocks between one and five AU: Pioneer 10 and 11, *Geophys. Res. Lett.*, *3*, 137.

Smith, E. J., and J. H. Wolfe (1977), Pioneer 10 and 11 observations of evolving solar wind streams and shocks beyond 1 AU, in *Study of Traveling Interplanetary Phenomena*, edited by M. Shea, D. F. Smart, and S. T. Wu, p. 227, D. Riedel, Hingham, Mass.

Szabo, A. (2005), Multi-spacecraft observations of interplanetary shocks, in *The Physics of Collisionless Shocks*, edited by G. Li, G. P. Zank, and C. T. Russell, p. 37, Am. Inst. of Phys., Melville, N. Y.

Toptyghin, I. N. (1980), Acceleration of particles by shocks in a cosmic plasma, *Space Sci. Rev.*, *26*, 157.

Torsti, J., et al. (1995), Energetic Particle Experiment ERNE, *Sol. Phys. 162*, 505.

Torsti, J., P. Mäkelä, E. Riihonen, and O. Saloniemi (2006), Great storm particle event on 2000 August 11 observed by SOHO ERNE, *Astrophys. J.*, *638*, 530.

Tylka, A., and M. A. Lee (2006), A model for spectral and compositional variability at high energies in large, gradual solar particle events, *Astrophys. J.*, *646*, 1319.

Volkmer, P. M., and F. M. Neubauer (1985), Statistical properties of fast magnetoacoustic shock waves in the solar wind between 0.3 AU and 1 AU, *Ann. Geophys.*, *3*, 1.

Winterhalter, D., E. J. Smith, M. E. Burton, N. Murphy, and D. J. McComas (1994), The heliospheric plasma sheet, *J. Geophys. Res.*, *99*, 6667.

Zhang, J., I. G. Richardson, D. F. Webb, N. Gopalswamy, E. Huttunen, J. Kasper, N. Nitta, W. Poomvises, B. J. Thompson, C.-C. Wu, S. Yashiro, and A. Zhukov (2007), Solar and interplanetary sources of major geomagnetic storms ($Dst \leq -100$ nT) in 1996–2004, *J. Geophys. Res.*, *112*, A12105, doi:10.1029/2007JA012332.

Zurbuchen, T. H., and I. G. Richardson (2006), In-situ solar wind and magnetic field signatures of interplanetary coronal mass ejections, *Space Sci. Rev.*, *123*, 31.

H. V. Cane and I. G. Richardson, Astroparticle Physics Laboratory, NASA Goddard Space Flight Center, Code 661, Greenbelt, MD 20771, USA. (hilary.cane@utas.edu.au; ian.g.richardson@nasa.gov)